RESEARCH ARTICLE

Figures and figure supplements

A drug repurposing approach reveals targetable epigenetic pathways in *Plasmodium vivax* hypnozoites

Steven P Maher *et al*.

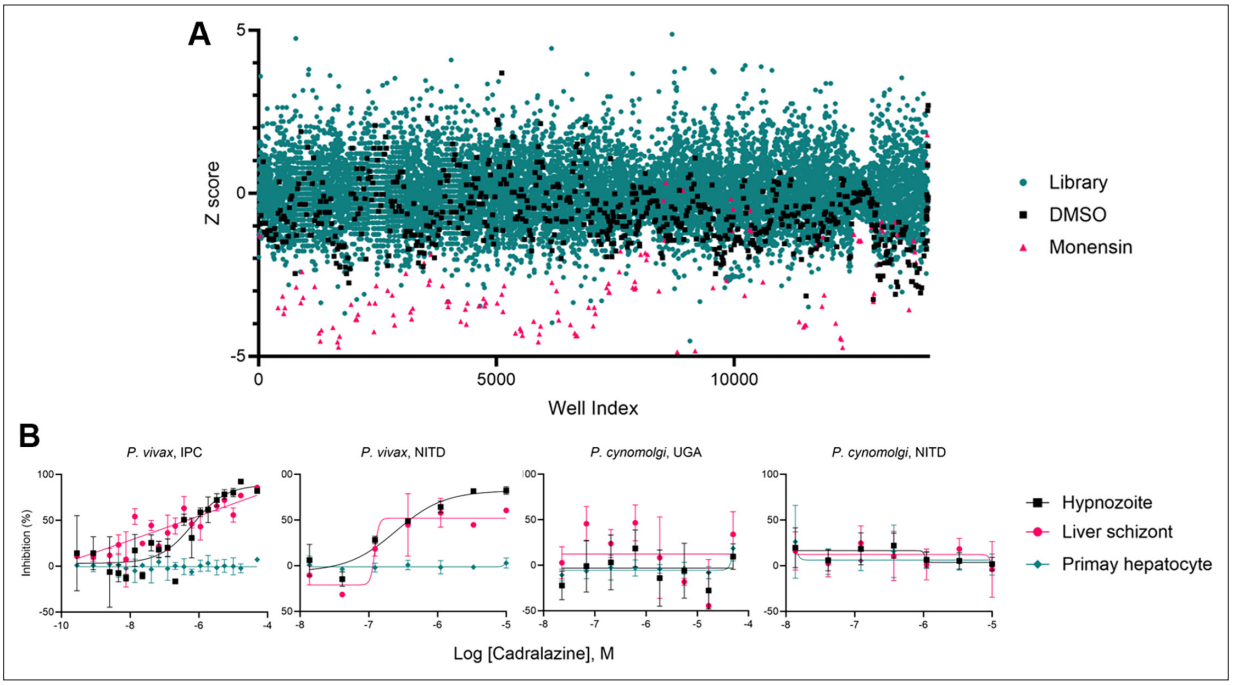

Figure 1. Hypnozonticidal hit detection and confirmation. (**A**) Index chart depicting the primary screen of the ReFRAME library against *P. vivax* hypnozoites in an 8-day assay. Hypnozoite counts were normalized by mean quantity per well for each plate (*Z*-score). Teal: library, black: DMSO, red: 1 μM monensin. (**B**) Dose–response curves for cadralazine against *P. vivax* and *P. cynomolgi* liver forms in 8-day assays at the IPC, UGA, and NITD. All replicate wells were plotted together from all independent experiments (n = 3 for *P. vivax* at IPC, n = 1 for *P. vivax* at NITD, n = 2 for *P. cynomolgi* at UGA, and n = 4 for *P. cynomolgi* at NITD), bars represent SEM.

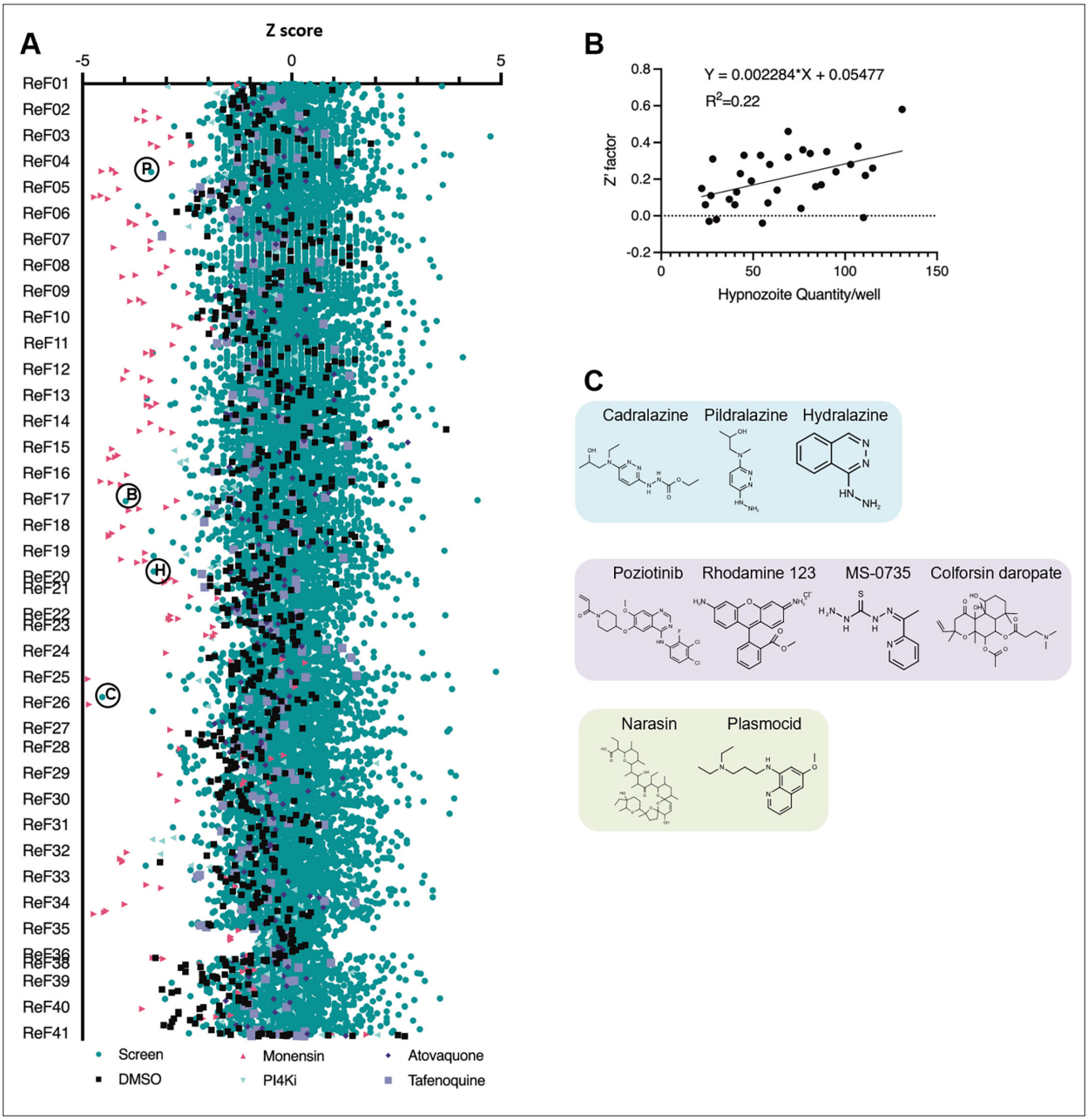

Figure 1—figure supplement 1. ReFRAME screen run detail and hit structures. (**A**) Index chart from ***Figure 1A*** with phosphatidylinositol 4-kinase inhibitor (PI4Ki) KDU691 or MMV390048, tafenoquine, and atovaquone controls added. Teal circle: library, black square: DMSO, pink triangle: 1 μM monensin, light green inverted triangle: 1 μM P4Ki, black diamond: 1 μM atovaquone, purple square: 10 μM tafenoquine. Some hits discussed in this report are noted with black circles; P: poziotinib, B: budralazine, H: hydralazine, C: cadralazine. (**B**) Simple linear regression correlating *Z*-factor with average hypnozoite count per well. (**C**) Structures of hits which confirmed to be active against *P. vivax* hypnozoites in dose–response assays; blue: hydralazine analogs, purple: other novel hits, green: re-discovery of compounds previously demonstrated to have hypnozonticidal activity in vitro or antirelapse activity in vivo.

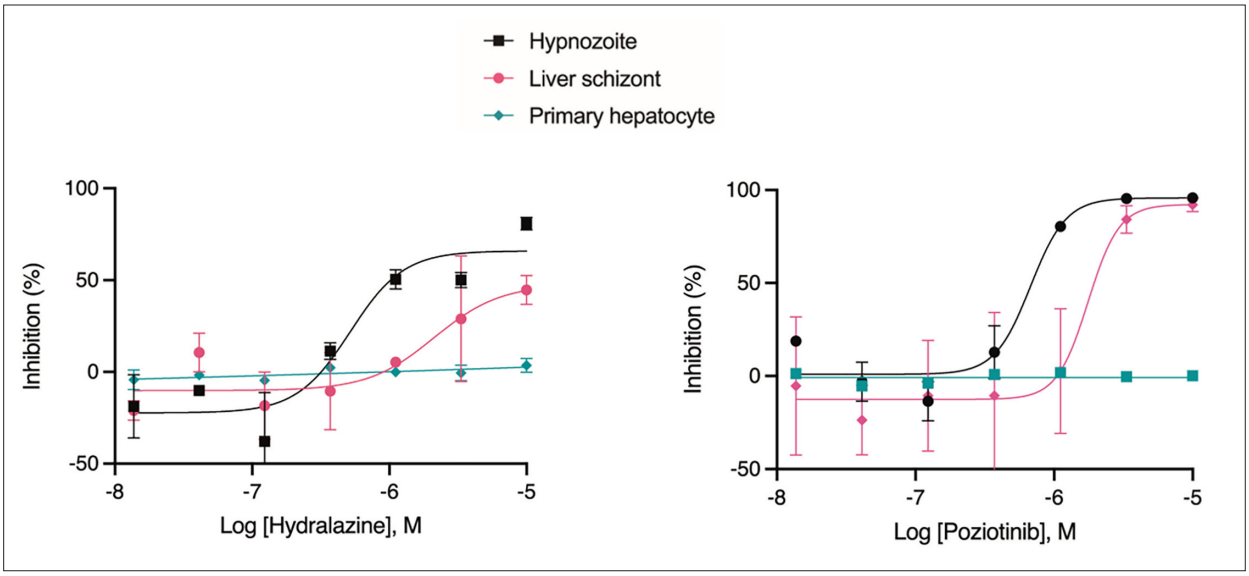

Figure 1—figure supplement 2. Select ReFRAME hits confirmed at Novartis Institute for Tropical Diseases (NITD). Dose–response curves for hydralazine and poziotinib against *P. vivax* liver forms assayed at NITD. All replicate wells were plotted together from a single independent experiment, bars represent SEM.

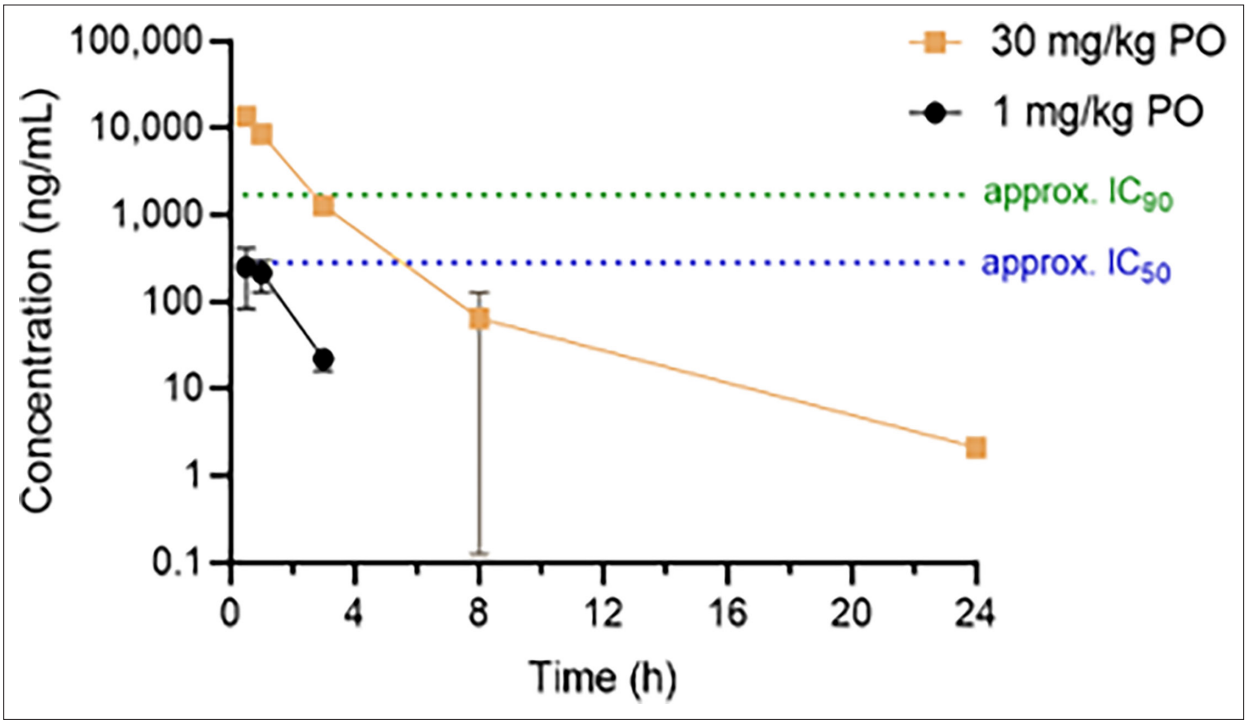

Figure 1—figure supplement 3. Pharmacokinetics of cadralazine in nonhuman primates. Mean plasma concentration of cadralazine was measured in three male rhesus macaques after oral dosing. Plasma was collected following a 1 mg/kg dose, and again following a 30 mg/kg dose. Bars represent SD. The approximate IC_{50} and IC_{90} from *P. vivax* hypnozoite assays are indicated.

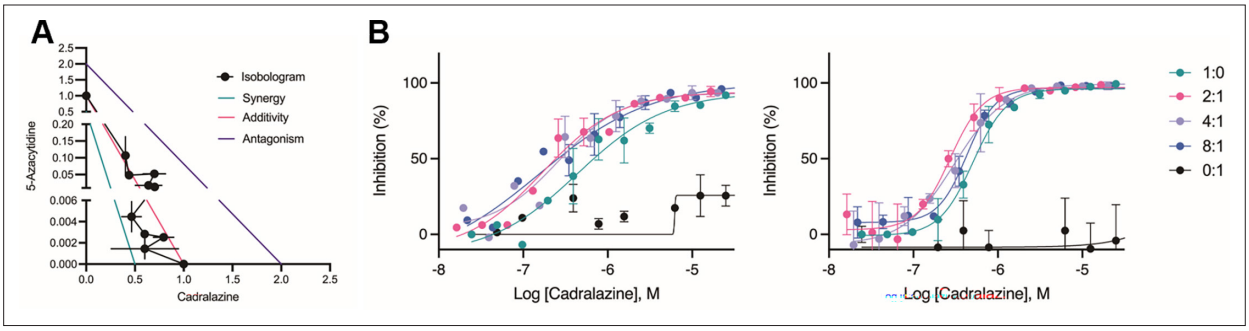

Figure 2. Synergistic effect of cadralazine and 5-azacytidine in *P. vivax* liver stage assays. (**A**) Isobologram of cadralazine and 5-azacytidine activity against hypnozoites in fixed ratios of 1:0, 8:1, 6:1, 4:1, 2:1, 1:1, 1:2, 1:4, 1:6, 1:8, and 0:1, bars represent SD of FICs from two independent experiments. (**B**) Dose–response curves for cadralazine at the most synergistic fixed ratios (2:1, 4:1, and 8:1) against hypnozoites. Cadralazine alone is represented as 1:0, 5-azacytidine alone is represented as 0:1 and plotted on the cadralazine chart for comparison. Left and right charts represent two independent experiments, bars represent replicate wells at each dose.

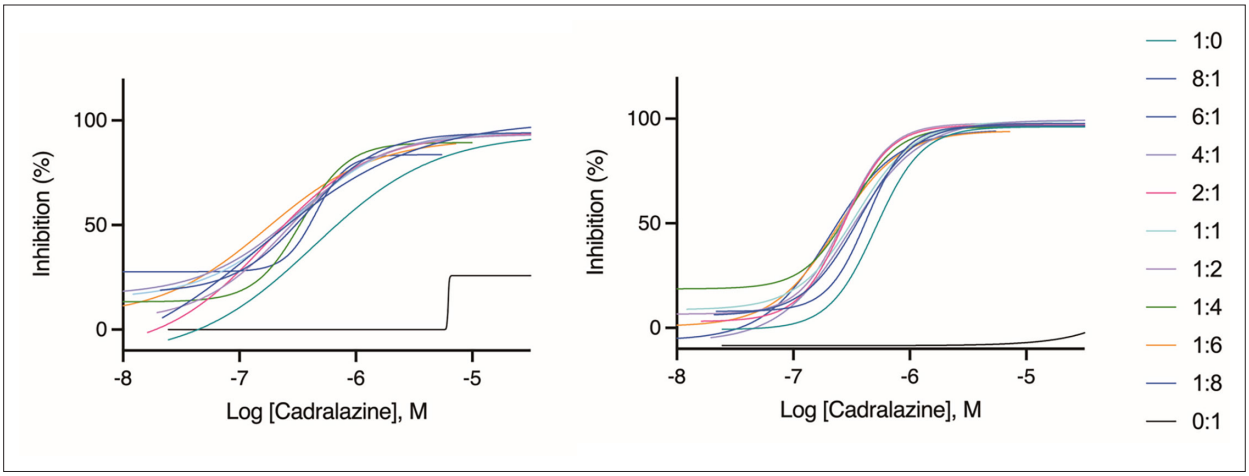

Figure 2—figure supplement 1. Synergistic effect of cadralazine and 5-azacytidine in *P. vivax* liver stage assays. Dose–response curves for cadralazine with all fixed ratios of 5-azacytidine against *P. vivax* hypnozoites. Cadralazine alone is represented as 1:0, 5-azacytidine alone is represented as 0:1 and plotted on the cadralazine chart for comparison. Left and right charts represent two independent experiments.

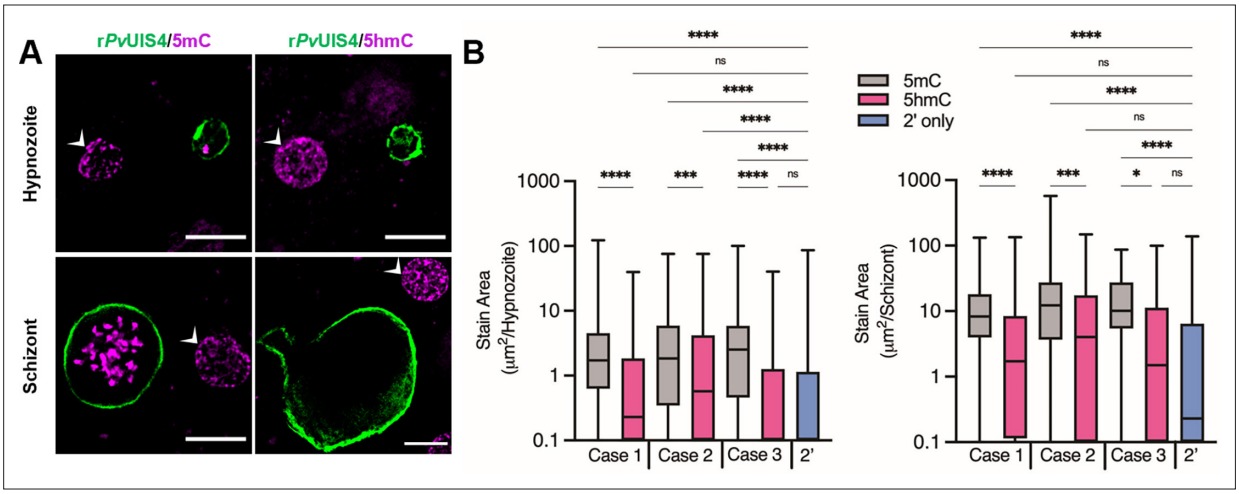

Figure 3. Cytosine modifications in *P. vivax* liver forms. (**A**) Immunofluorescent imaging of a 5mC-positive (left) or 5hmC-negative (right) *P. vivax* hypnozoite (top) and schizont (bottom) at day 6 post-infection. White arrows indicate hepatocyte nuclei positive for 5mC or 5hmC. Bars represent 10 µm. (**B**) High-content quantification of 5mC or 5hmC stain area within hypnozoites or schizonts from sporozoites generated from three different *P. vivax* cases. Significance determined using Kruskal–Wallis tests, for hypnozoites $H(7) = 194.3$, $p < 0.0001$, for schizonts $H(7) = 88.66$, $p < 0.0001$, with Dunn's multiple comparisons, *p < 0.05, ***p < 0.001, ****p < 0.0001, ns = not significant. Line, box, and whiskers represent median, upper and lower quartiles, and minimum-to-maximum values, respectively, of all hypnozoites ($177 \leq n \leq 257$) or all schizonts ($30 \leq n \leq 142$) in culture for each case, 2' indicates a secondary stain only control.

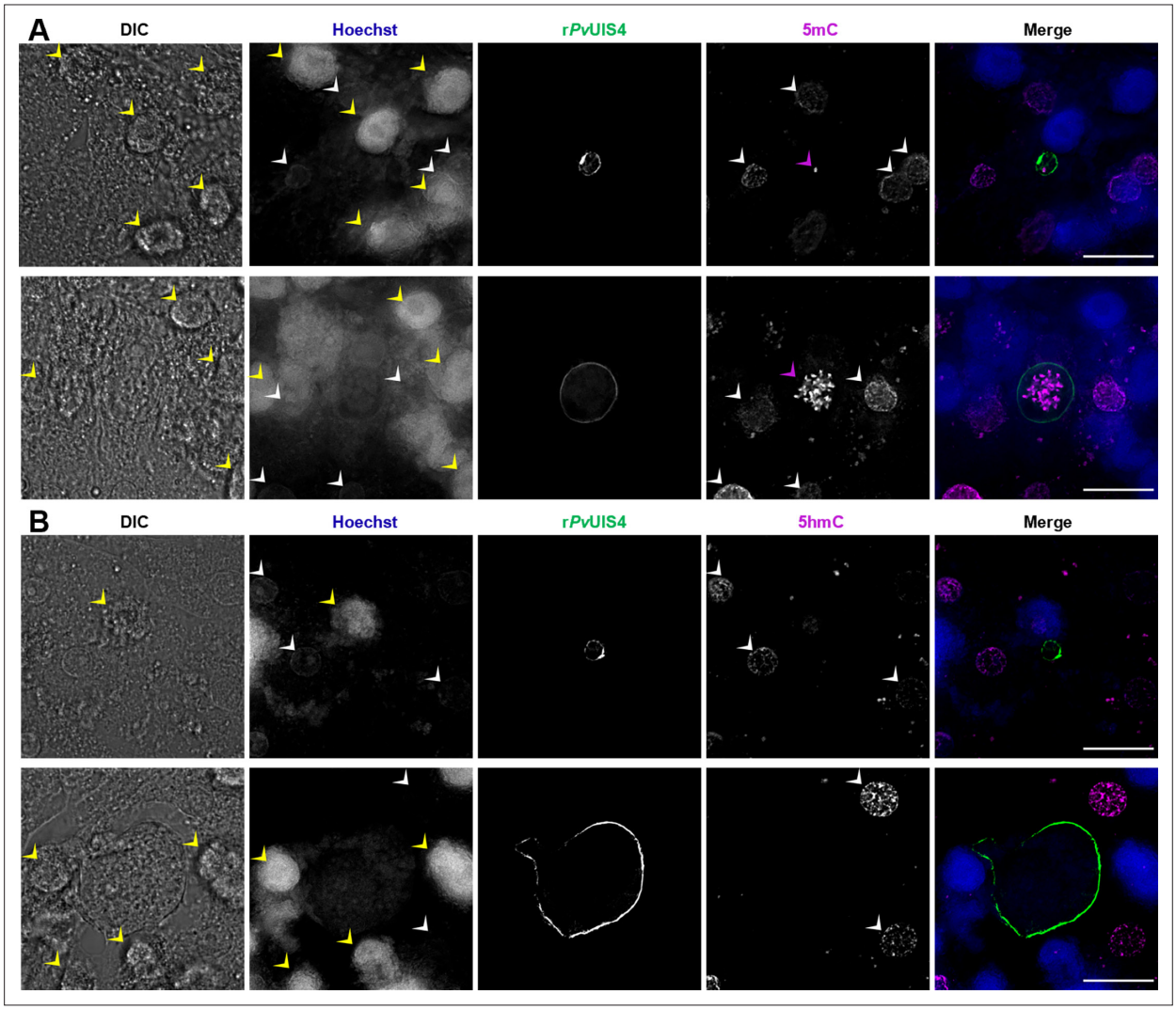

Figure 3—figure supplement 1. Cytosine modifications in *P. vivax* liver forms, full panels from case 1 (expanded from ***Figure 3***). (**A**) Immunofluorescent imaging of a 5mC-positive *P. vivax* hypnozoite (top) and schizont (bottom) at day 6 post-infection. (**B**) Immunofluorescent imaging of a 5hmC-negative *P. vivax* hypnozoite (top) and schizont (bottom) at day 7 post-infection. Yellow arrows indicate autofluorescence in the blue channel associated with cell debris above the hepatocyte monolayer. White arrows indicate hepatocyte nuclei which are dimly stained with Hoechst 33342 and positive for 5mC or 5hmC. Purple arrows indicate 5mC-positive foci within the parasite. Bars represent 20 μm.

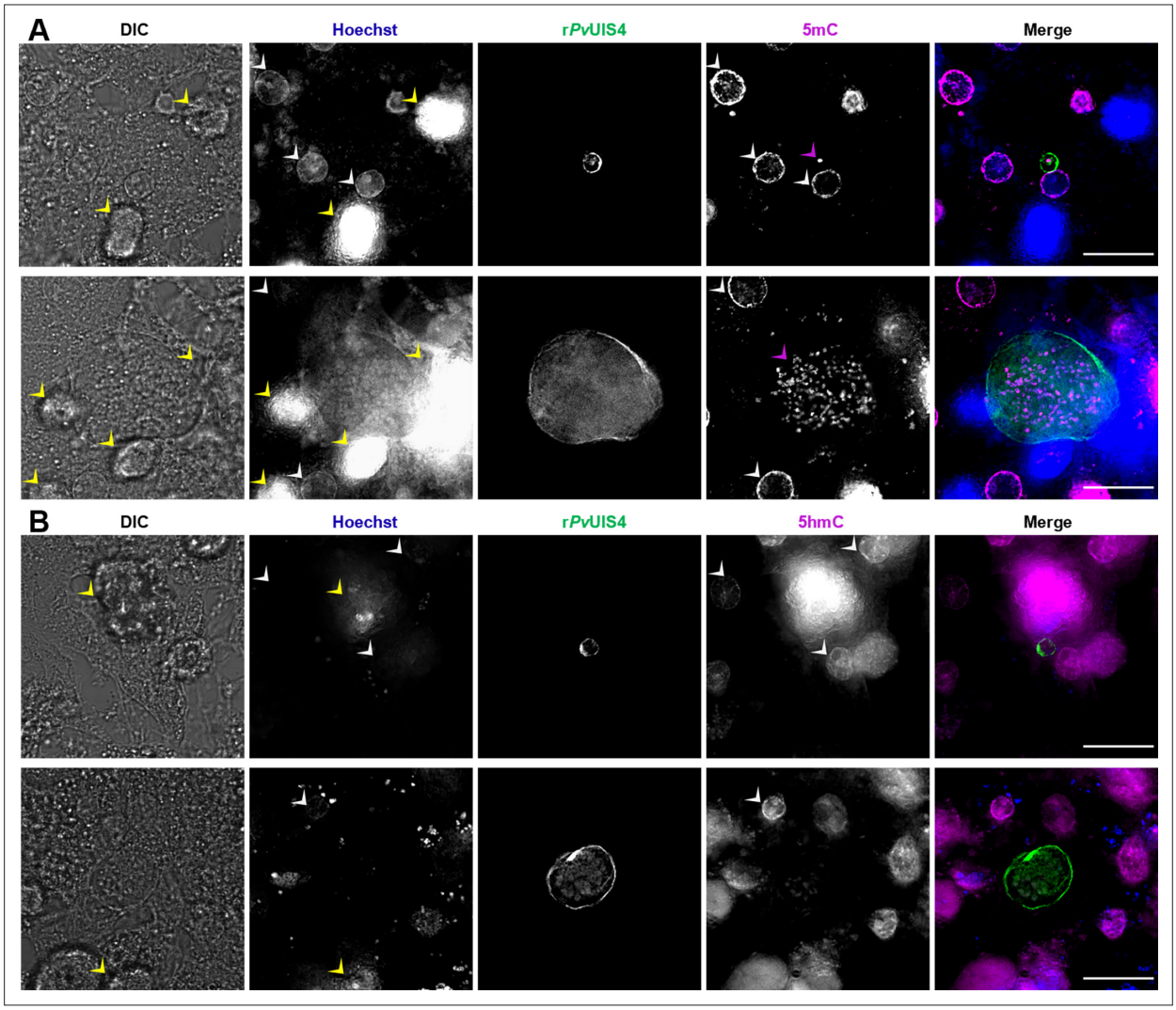

Figure 3—figure supplement 2. Cytosine modifications in *P. vivax* liver forms, full panels from case 2. (**A**) Immunofluorescent imaging of a 5mC-positive *P. vivax* hypnozoite (top) and schizont (bottom) at day 6 post-infection. (**B**) Immunofluorescent imaging of a 5hmC-negative *P. vivax* hypnozoite (top) and schizont (bottom) at day 7 post-infection. Yellow arrows indicate autofluorescence in the blue channel associated with cell debris above the hepatocyte monolayer. White arrows indicate hepatocyte nuclei which are dimly stained with Hoechst 33342 and positive for 5mC or 5hmC. Purple arrows indicate 5mC-positive foci within the parasite. Bars represent 20 μm.

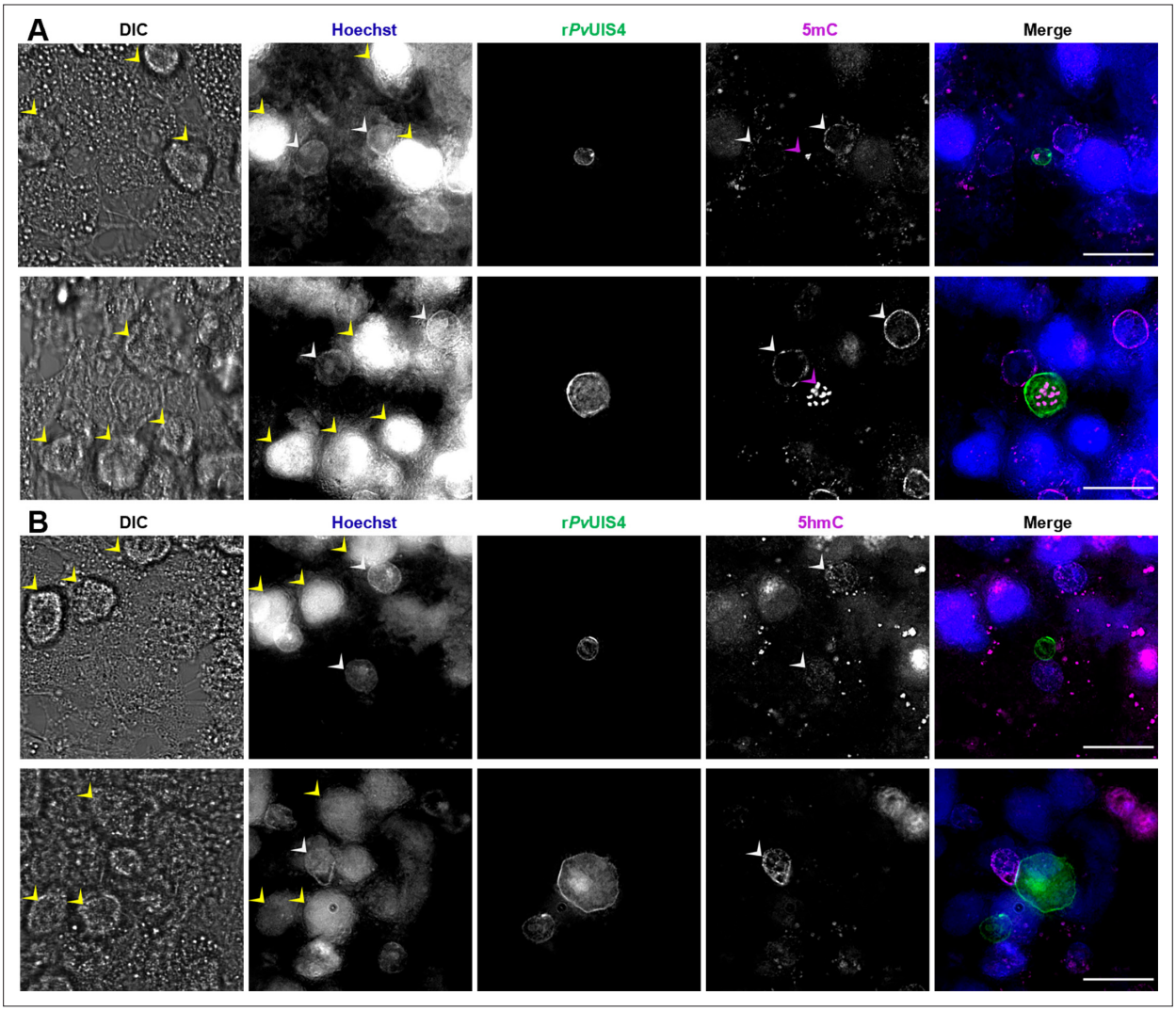

Figure 3—figure supplement 3. Cytosine modifications in *P. vivax* liver forms, full panels from case 3. (**A**) Immunofluorescent imaging of a 5mC-positive *P. vivax* hypnozoite (top) and schizont (bottom) at day 6 post-infection. (**B**) Immunofluorescent imaging of a 5hmC-negative *P. vivax* hypnozoite (top) and schizont (bottom) at day 7 post-infection. Yellow arrows indicate autofluorescence in the blue channel associated with cell debris above the hepatocyte monolayer. White arrows indicate hepatocyte nuclei which are dimly stained with Hoechst 33342 and positive for 5mC or 5hmC. Purple arrows indicate 5mC-positive foci within the parasite. Bars represent 20 μm.

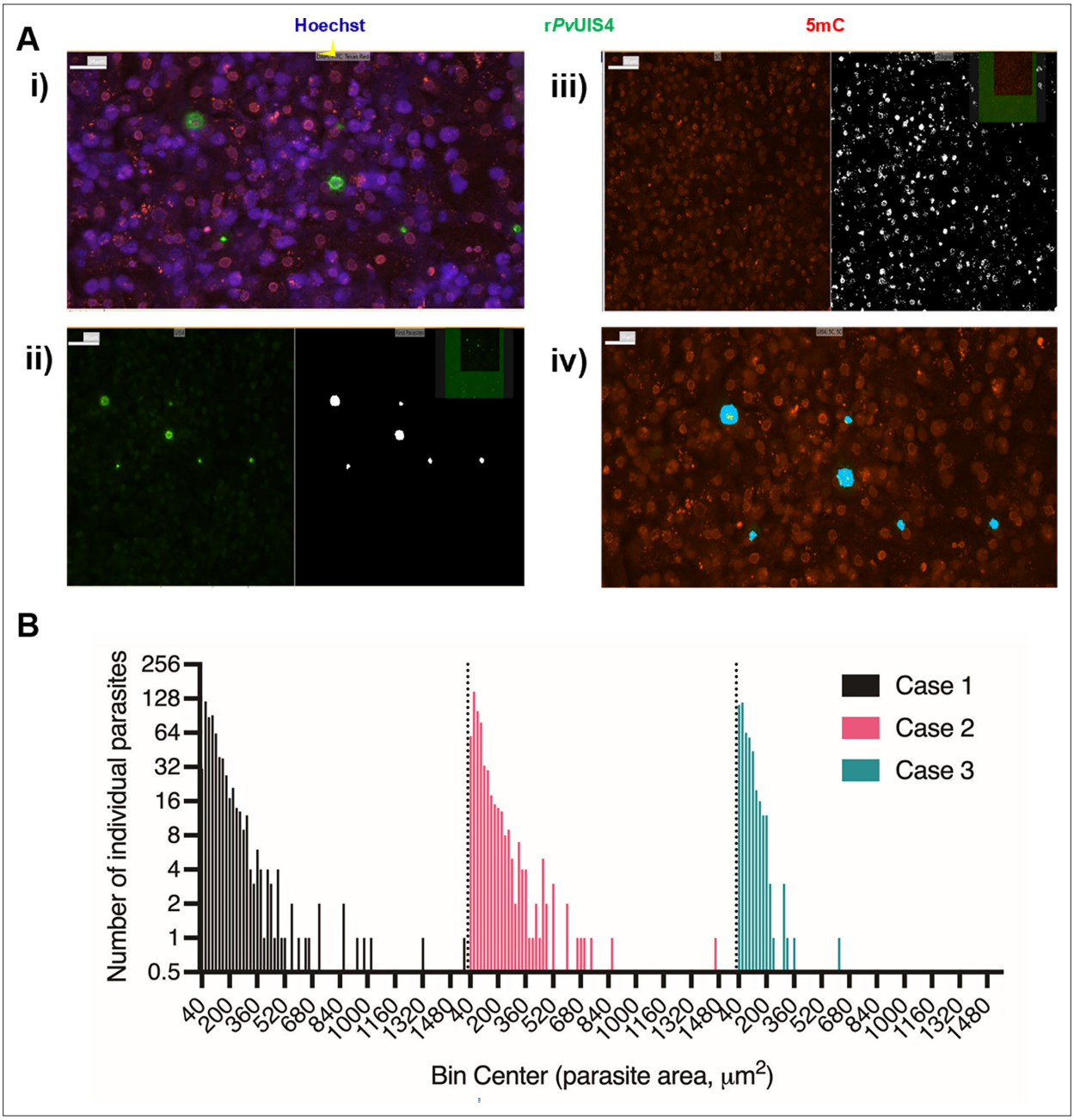

Figure 3—figure supplement 4. High-content analysis of cytosine modifications and *P. vivax* liver stage population metrics. (**A**) Masks used to quantify parasite area and 5mC or 5hmC signal, (i) raw image taken with a 20x objective, (ii) Mask for *P. vivax* liver stages, (iii) mask for 5mC or 5hmC signal, and (iv) intersection of parasite mask (light blue) and 5mC or 5hmC signal mask (yellow), leading to quantified area of signal per form. (**B**) Histogram of growth area all parasites quantified for Cases 1, 2, and 3 in ***Figure 3***. Hypnozoites were classified as forms with an area of 125 μm^2 and smaller.

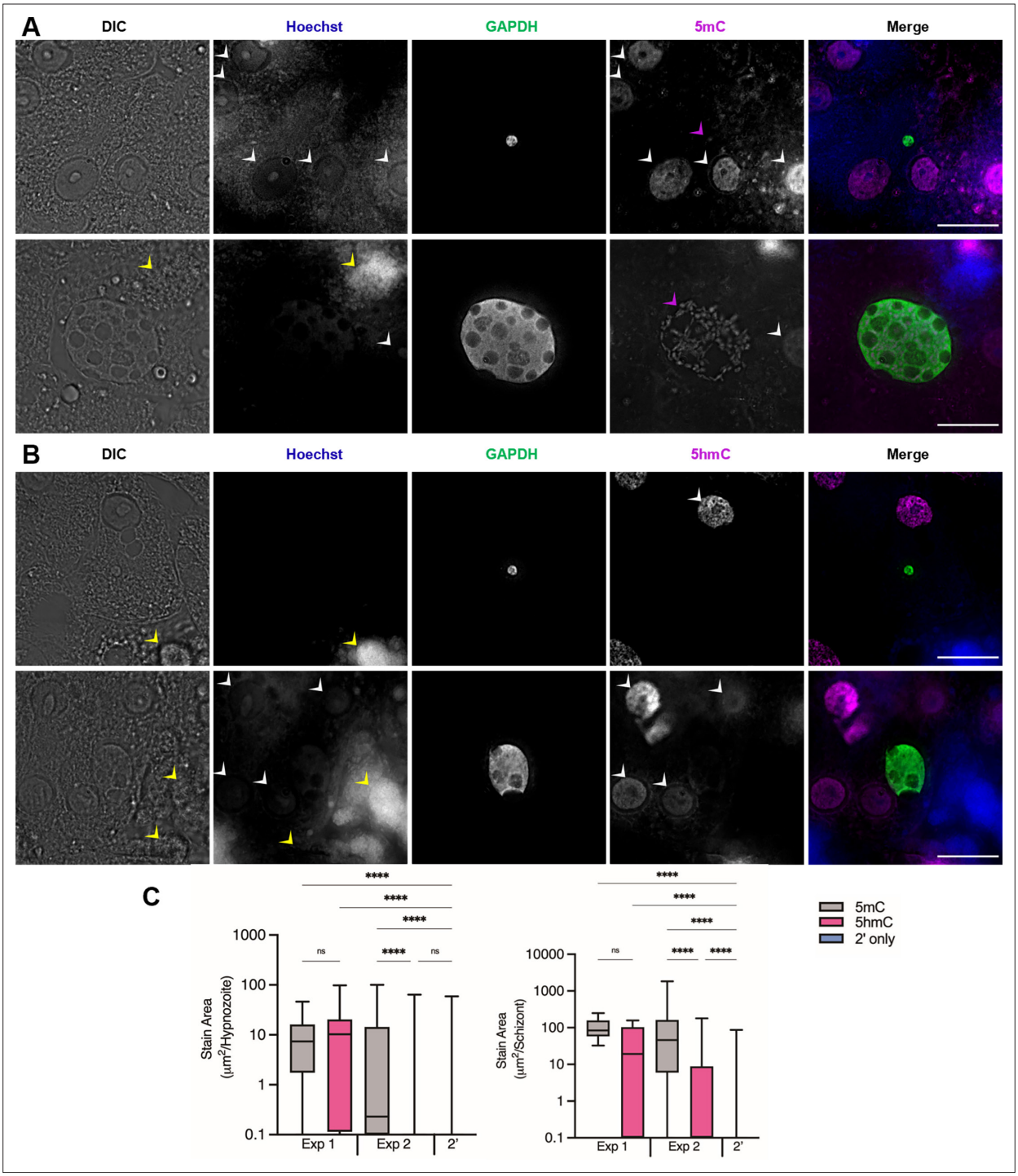

Figure 3—figure supplement 5. Cytosine modifications in *P. cynomolgi* M/B strain liver forms. (**A**) Immunofluorescent imaging of a 5mC-positive *P. cynomolgi* hypnozoite (top) and schizont (bottom) at day 8 post-infection. (**B**) Immunofluorescent imaging of a 5hmC-negative *P. cynomolgi* hypnozoite (top) and schizont (bottom) at day 8 post-infection. Yellow arrows indicate autofluorescence in the blue channel associated with cell debris above the hepatocyte monolayer. White arrows indicate hepatocyte nuclei which are dimly stained with Hoechst 33342 and positive for 5mC or 5hmC. Purple arrows indicate 5mC-positive foci within the parasite. Bars represent 20 µm. (**C**) High-content quantification of 5mC or 5hmC stain area within hypnozoites or schizonts. Experiment 1 was fixed at day 8 post-infection, Experiment 2 was fixed at day 12 post-infection. Significance was determined using Kruskal–Wallis tests for hypnozoites and schizonts, with Dunn's multiple comparisons, ****$p < 0.0001$, ns = not significant. Line, box, and whiskers represent median, upper and lower quartiles, and minimum-to-maximum values, respectively, of all hypnozoites ($124 \leq n \leq 712$) or all schizonts ($7 \leq n \leq 581$) in culture, 2' indicates a secondary stain only control. Images in **A**, **B** are from Experiment 1.

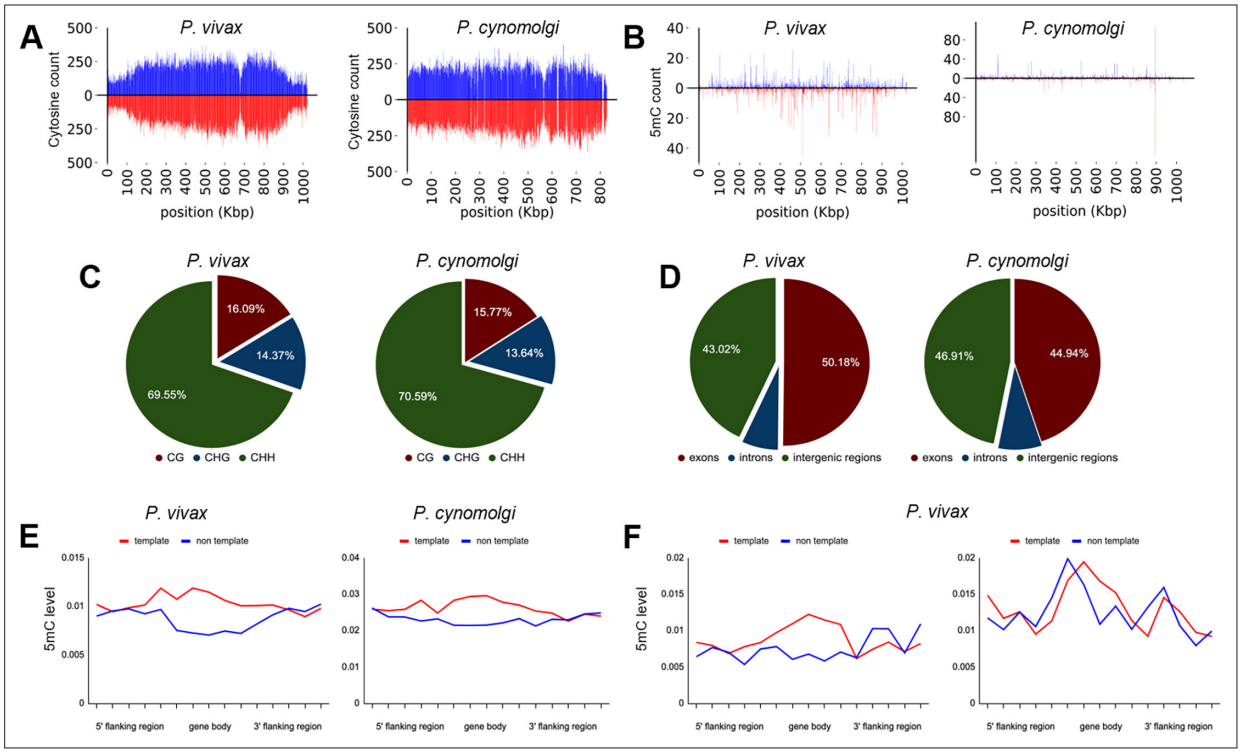

Figure 4. Density of cytosine and methylated cytosine (5mC) in sporozoites. (**A**) CG content of chromosome 1 for *P. vivax* and *P. cynomolgi*. The total number of cytosines was quantified on each strand using 1 kbp long non-overlapping windows. (**B**) The total number of methylated cytosines was quantified on each strand using 1 kbp long non-overlapping windows. (**C**) The number of 5mC present in all possible contexts (CG, CHG, and CHH) quantified throughout the genome of *P. vivax* and *P. cynomolgi*. (**D**) Repartitioned 5mC quantity within different compartments of the genome in *P. vivax* and *P. cynomolgi*. (**E**) Strand specificity of 5mC for all genes in *P. vivax* and *P. cynomolgi*. Flanking regions and gene bodies were divided into five bins, and the methylation level of each bin was averaged among all genes. Red: template strand, blue: non-template strand. (**F**) The previously reported mRNA abundance of *P. vivax* sporozoites was retrieved (***Antonova-Koch et al., 2018***) and genes ranked. The 5mC levels in 5′ flanking regions, gene bodies, and 3′ flanking regions were placed into five bins and are shown for highly expressed (90th percentile, left) and weakly expressed (10th percentile, right) genes. Red: template strand, blue: non-template strand.

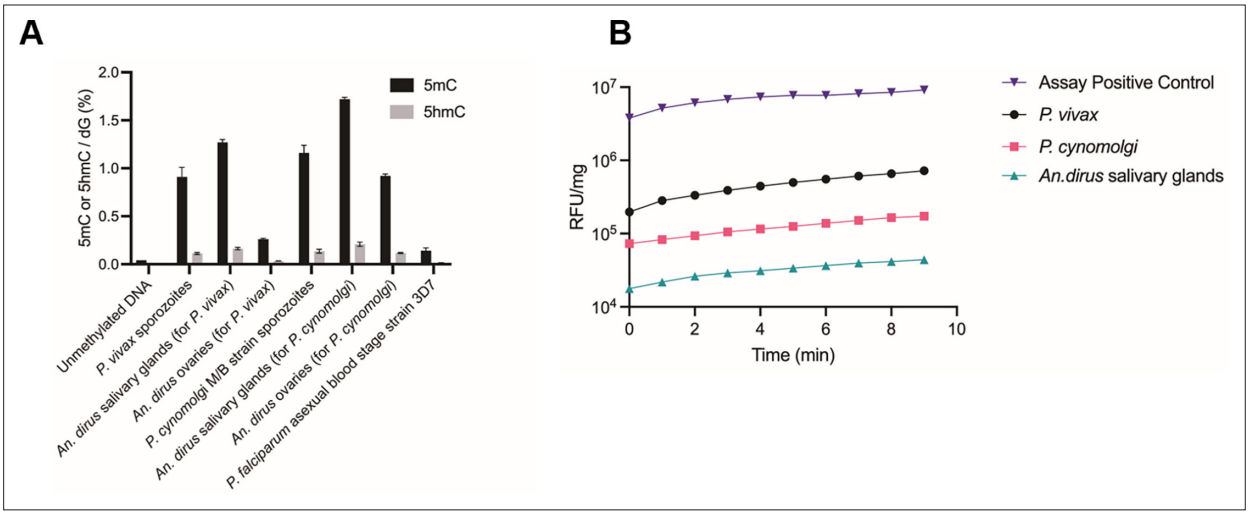

Figure 4—figure supplement 1. Measurement of DNA methylation and DNA methyltransferase (DNMT) in *P. vivax* and *P. cynomolgi* sporozoites. (**A**) Liquid chromatography–tandem mass spectrometry (LC–MS/MS) analysis of 5mC or 5hmC from enzymatically digested gDNA from *P. vivax* sporozoites, *P. cynomolgi* sporozoites, and *P. falciparum* blood stage parasites, as well as negative controls including uninfected mosquito salivary glands and ovaries from the same colony of mosquitoes used to generate the respective sporozoites. Bars represent SD of two independent experiments. (**B**) DNMT activity measured from nuclear extracts of *P. vivax* sporozoites, *P. cynomolgi* sporozoites, and uninfected mosquito salivary glands using the Epiquick DNMT activity assay. Data are from a single experiment.

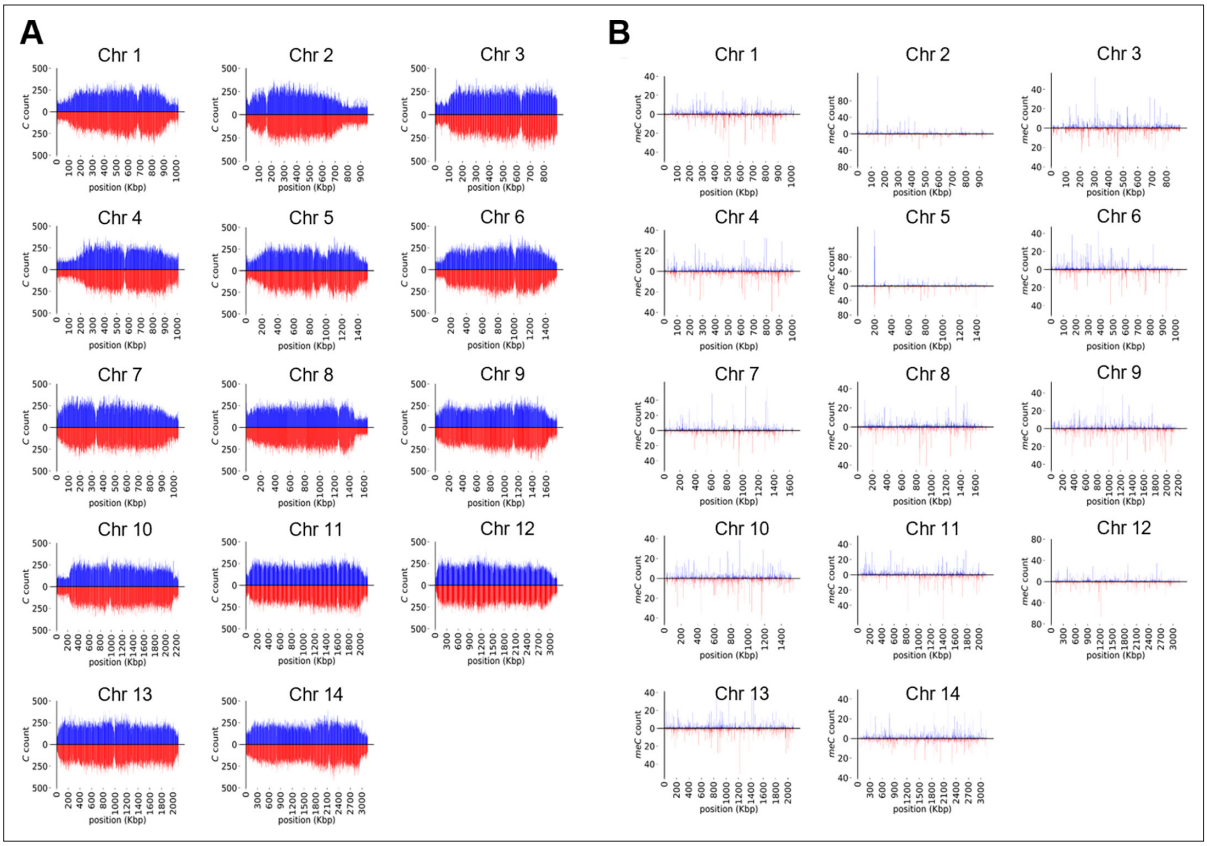

Figure 4—figure supplement 2. Cytosine and methylation density plots for *P. vivax* sporozoites. (**A**) CG content of chromosome 1–14 (Chr 1–14). The total number of cytosines quantified on each strand using 1 kb long non-overlapping windows. (**B**) The total number of methylated cytosines quantified on each strand using 1 kb long non-overlapping windows.

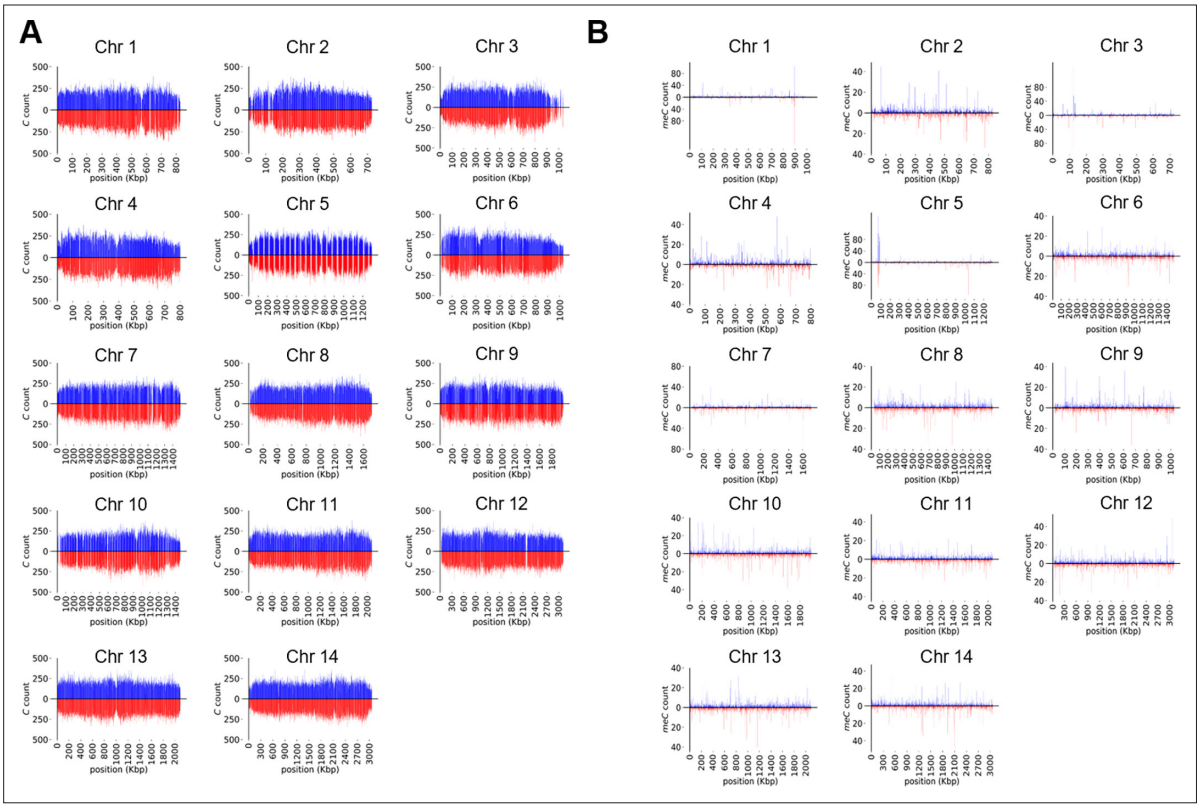

Figure 4—figure supplement 3. Cytosine and methylation density plots for *P. cynomolgi* sporozoites. (**A**) CG content of chromosome 1–14 (Chr 1–14). The total number of cytosines quantified on each strand using 1 kb long non-overlapping windows. (**B**) The total number of methylated cytosines quantified on each strand using 1 kb long non-overlapping windows.

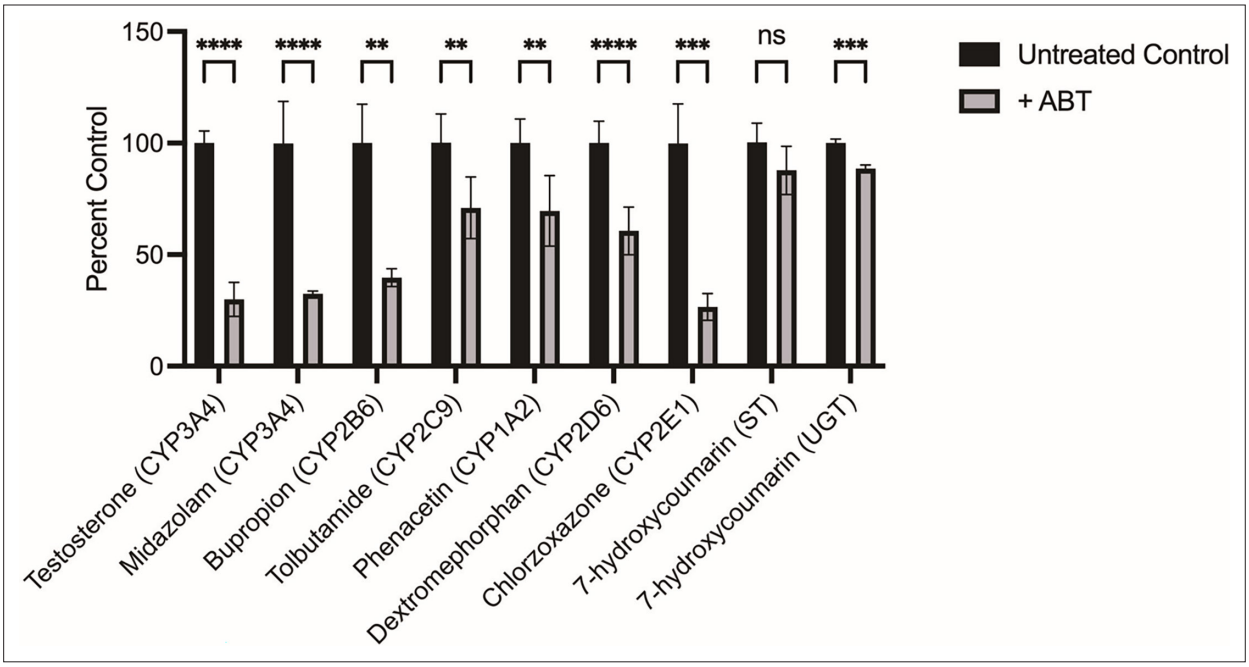

Figure 5. Characterization of primary human hepatocyte (PHH) metabolism following 1-aminobenzotriazole (1-ABT) treatment. PHH lot BGW was seeded in 384-well plates and cultured for 7 days before treatment with 100 μM 1-ABT for 1 hr, followed by addition of substrates for 1 hr and collection for analysis by mass spectrometry. Data are combined from two independent experiments, bars represent SD of all replicates. Significance determined by Student's *t* tests, ****p < 0.0001, ***p < 0.001, **p < 0.01, ns, not significant.

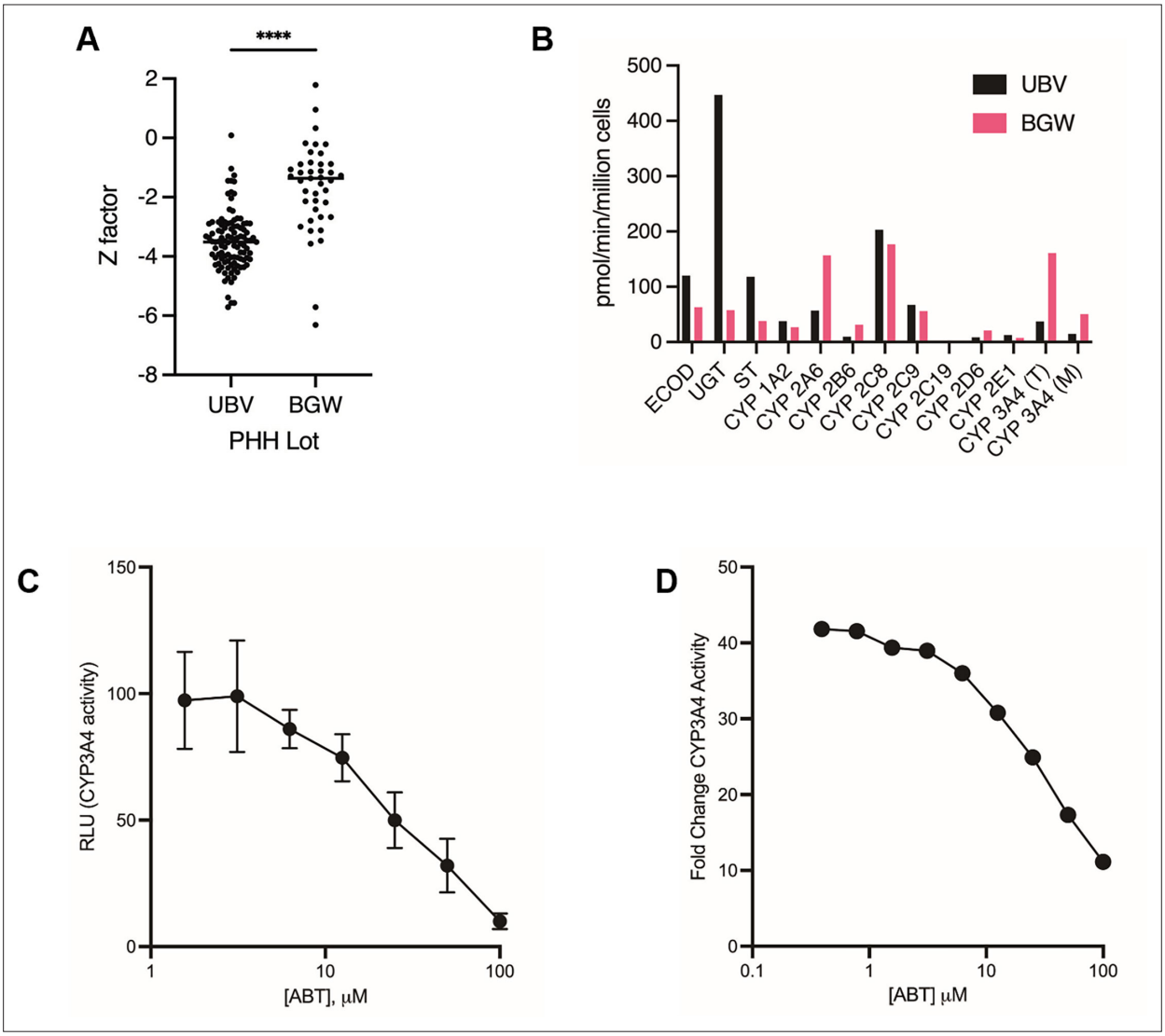

Figure 5—figure supplement 1. Monensin activity in all control wells based on primary human hepatocyte (PHH) lot. (**A**) Initially, the ReFRAME was screened with cryopreserved vials of a specific lot of PHH, UBV. Screening continued with a new lot, BGW, once the supply of UBV vials was exhausted. The activity of monensin was significantly reduced in wells with BGW versus UBV PHH. A Mann–Whitney test indicates the difference was statistically significant, $U(N_{UBV} = 105, N_{BGW} = 41) = 552$, $z = -2.15$, ****$p < 0.0001$. (**B**) Metabolic activity panel for PHH lots UBV and BGW performed as part of regular quality control at the vendor (BioIVT). ECOD: 7-ethoxycoumarin *O*-deethylation, UGT: 7-hydroxycoumarin glucuronidation, ST: 7-hydroxycoumarin sulfation, CYP 1A2: phenacetin *O*-deethylation, CYP 2A6: coumarin 7-hydroxylation, CYP 2B6: bupropion hydroxylation, CYP 2C8: amodiaquine *N*-desethylation, CYP 2C9: tolbutamide methyl-hydroxylation, CYP 2C19: *S*-mephenytoin 4′-hydroxylation, CYP 2D6: dextromethorphan *O*-demethylation, CYP 2E1: chlorzoxazone 6-hydroxylation, CYP 3A4 (T): testosterone 6β-hydroxylation, CYP 3A4 (M): midazolam 1-hydroxylation. (**C**) PHH lot BGW was seeded into 384-well plates and cultured for 7 days before addition of a dilution series of 1-aminobenzotriazole (1-ABT) in media. Cytochrome P450 3A4 activity (CYP3A4) was measured using luciferin-IPA (Promega). RLU: relative luminescence units. Bars represent SD of quadruplicate wells. Data are representative of two independent experiments. (**D**) PHH lot BGW was cultured in 384-well plates before addition of 25 μM rifampicin in media on days 4 and 6 to induce CYP3A4 expression. At day 7 post-seed, CYP3A4 activity was measured by adding luciferin-IPA and a dilution series of 1-ABT in media. Fold change was calculated based on matching uninduced controls. Data are from one independent experiment.

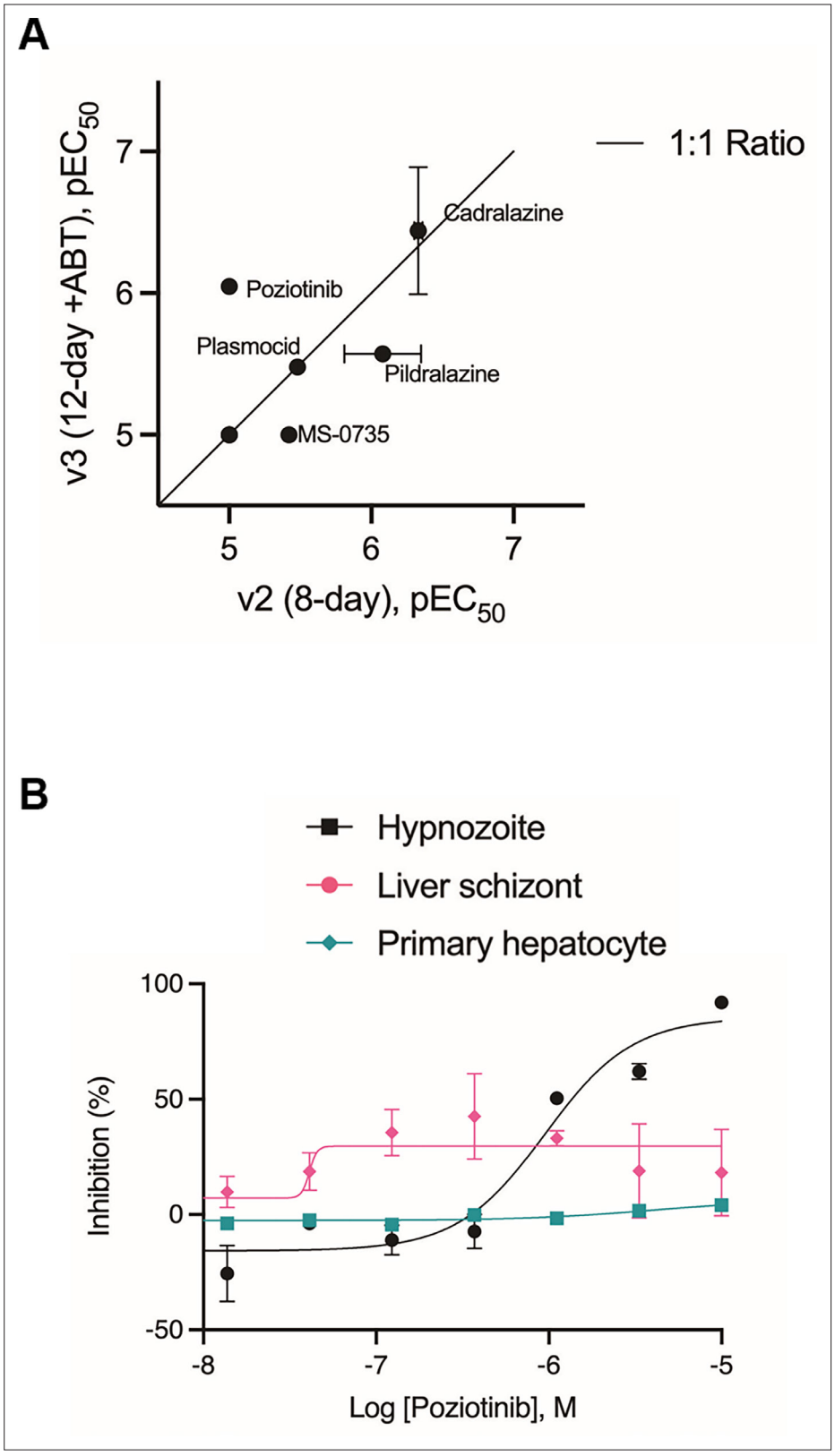

Figure 5—figure supplement 2. ReFRAME hits re-confirmed in a *P. vivax* 12-day 1-aminobenzotriazole (1-ABT) assay. (**A**) Hypnozonticidal potency comparison of 12 ReFRAME hits in 8- and 12-day 1-ABT dose–response confirmation assays. Cadralazine, plasmocid, and pidralazine potencies were unaffected by assay version, while MS-0735 was less potent, and poziotinib was more potent, in the 12-day 1-ABT assay. Budralazine, dramedilol,

Figure 5—figure supplement 2 continued on next page

Figure 5—figure supplement 2 continued

RGH-5526, dihydralazine, todralazine, endralazine, and mopidralazine were inactive (pEC_{50} <5) regardless of assay version. (**B**) Dose–response chart of poziotinib activity in the 12-day 1-ABT assay, pEC_{50} against hypnozoites = 6.05. Bars represent SEM.

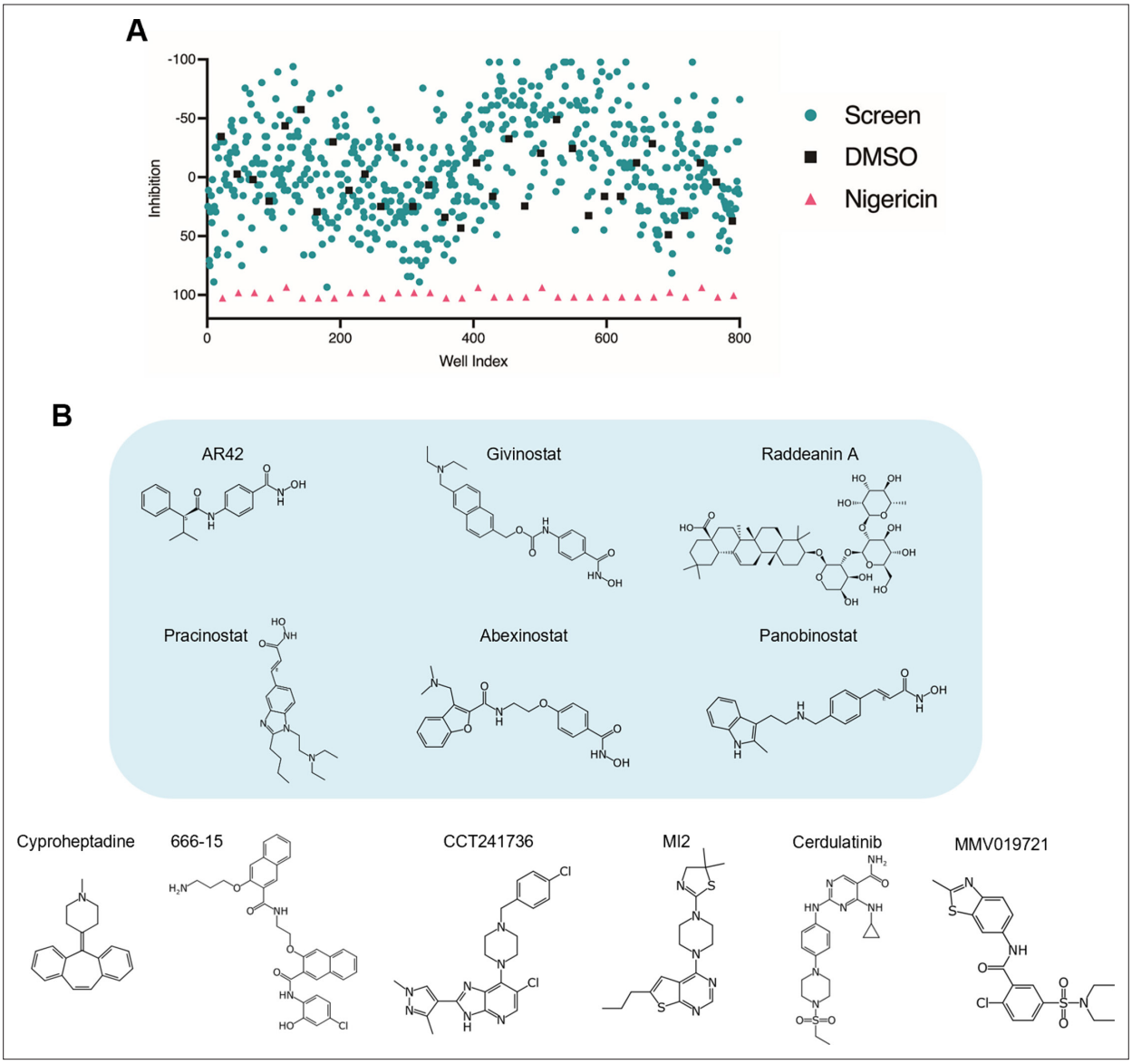

Figure 5—figure supplement 3. Epigenetic inhibitor library screen and hits. (**A**) Index chart of an epigenetic inhibitor library screened against *P. vivax* hypnozoites in a v3 (12-day 1-aminobenzotriazole [1-ABT]) assay. Teal circle: library, black square: DMSO, pink triangle: 200 nM nigericin. (B) Structures of epigenetic inhibitor hits which were confirmed to be active against *P. vivax* hypnozoites in dose–response assays; blue: histone deacetylase inhibitors.

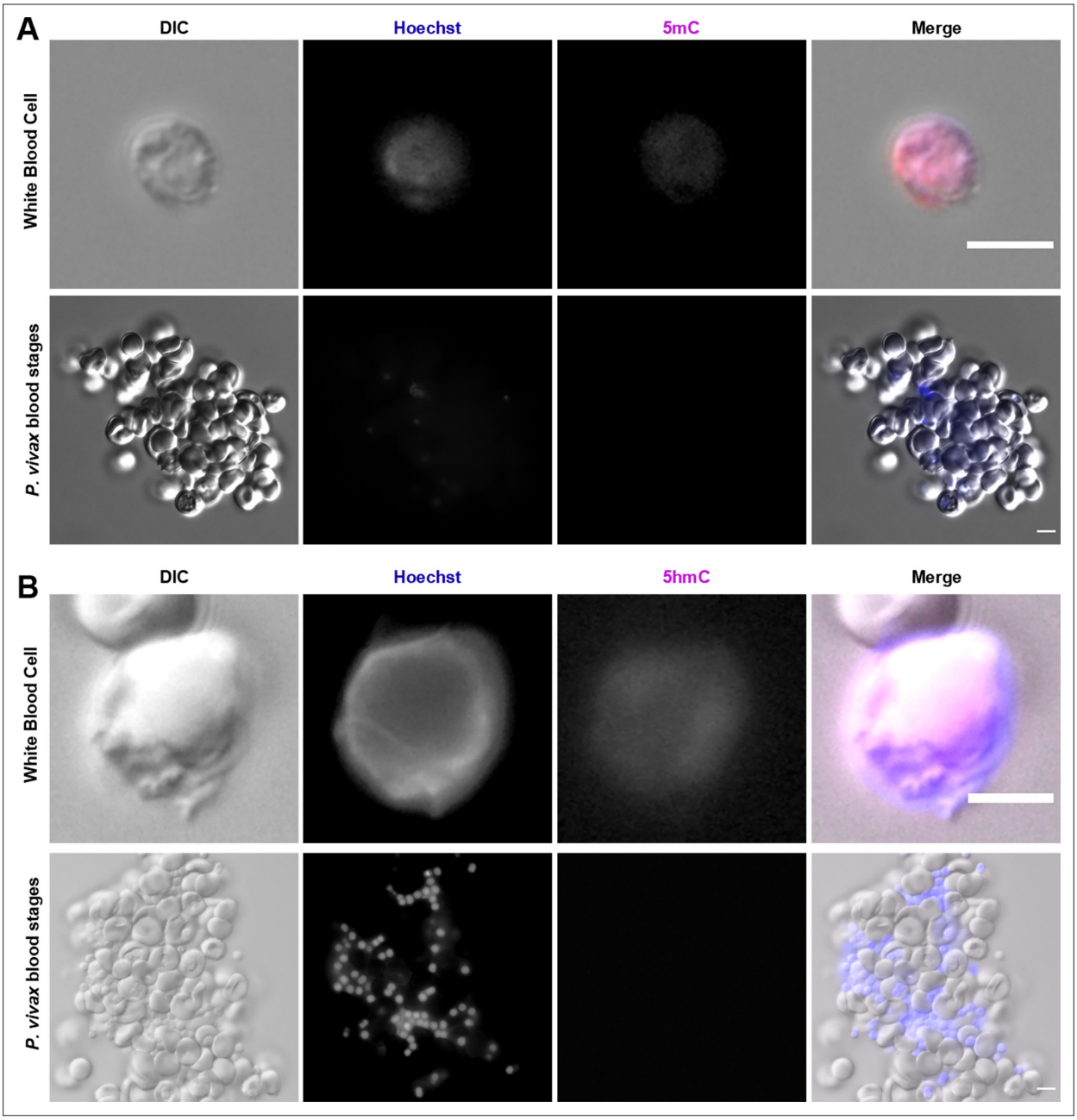

Appendix 1—figure 1. Cytosine modification in *P. vivax* blood stages. (**A**) *P. vivax* blood stages from patient isolates appeared negative when stained with 5mC. A white blood cell positive for 5mC serves as a stain control. (**B**) *P. vivax* blood stages from patient isolates appeared negative when stained with 5hmC. A white blood cell positive for 5hmC serves as a stain control. Bars represent 10 µm.